

Contrast discrimination with sinusoidal gratings of different spatial frequency

C. M. Bird

Department of Neuropsychology, The National Hospital, Queen Square, London WC1N 3BG, UK

G. B. Henning

The Institute of Cognitive Neuroscience, London, WC1N 3AR, UK

F. A. Wichmann

Max-Planck-Institut für biologische Kybernetik, Spemannstraße 38, D-72076 Tübingen, FRG

Received August 31, 2001; revised manuscript received January 18, 2002; accepted January 23, 2002

The detectability of contrast increments was measured as a function of the contrast of a masking or “pedestal” grating at a number of different spatial frequencies ranging from 2 to 16 cycles per degree of visual angle. The pedestal grating always had the same orientation, spatial frequency, and phase as the signal. The shape of the contrast-increment threshold versus pedestal contrast (TvC) functions depends on the performance level used to define the “threshold,” but when both axes are normalized by the contrast corresponding to 75% correct detection at each frequency, the TvC functions at a given performance level are identical. Confidence intervals on the slope of the rising part of the TvC functions are so wide that it is not possible with our data to reject Weber’s law. © 2002 Optical Society of America

OCIS codes: 330.1880, 330.5000, 330.5510, 330.7310.

1. INTRODUCTION

Contrast-discrimination experiments provide one means of studying the visual system’s response at suprathreshold contrast. Since the seminal study of Campbell and Robson¹ suggesting that the visual system is comprised of spatial-frequency-selective channels, much of the work on contrast discrimination has been carried out with sinusoidal stimuli in order to investigate contrast transduction and/or gain-control mechanisms operating within a single channel.^{2,3} While subsequent research has cast doubt on the notion of linear and independent channels,^{4,5} the multichannel model still captures many aspects of early spatial vision, and, even in nonlinear systems, results with sinusoidal stimuli remain interesting.

In standard, two-alternative forced-choice (2AFC) contrast-discrimination experiments, observers are typically required to discriminate between two sinusoidal gratings that differ only in their contrast. The grating of lower contrast is sometimes called the “pedestal” and sometimes the “masking grating” or “masker.” The observers are asked to choose the interval in which a “signal” grating is added to the pedestal. When the signal and pedestal gratings are in phase, the addition of the signal produces only an increase in contrast, so the observers’ task can also be described as choosing the interval containing the grating of higher contrast. With in-phase addition, the contrast increment is equal to the contrast of the signal.

The results of contrast-discrimination experiments are normally represented by plotting the discrimination

“threshold”—the signal contrast required for an arbitrarily chosen proportion of correct responses—against the pedestal contrast. Both axes are usually logarithmic. The resulting function is sometimes referred to as the threshold-versus-contrast (TvC) function and sometimes, because of its shape, the “dipper” function. With increasing pedestal contrast, the threshold first decreases before rising approximately linearly on log–log coordinates.^{6,7} The improvement in detection performance is called the pedestal, or dipper, effect. The effect is also found in hearing.^{8–10} In hearing, as well as in vision, the effect disappears when the signal and pedestal are presented in quadrature.¹¹

The dipper shape has been explained by models of sub-threshold summation,¹² energy detection (in hearing^{10,13}), uncertainty,^{14,15} divisive contrast–gain control,¹⁶ and most recently by a divisive gain-control model coupled with energy-dependent noise.¹⁷ Discrimination among the various models is sometimes based on the slope of the rising part of the TvC function usually on the basis of a single performance contour. However, despite some agreement as to general shape of the TvC function, there is considerable uncertainty about its shape over the rising part of its course and its dependence on spatial frequency. It has been of some interest to know whether contrast discrimination obeys Weber’s law.

A survey³ of fifteen studies of contrast discrimination reported that eight found Weber’s law and seven did not. The studies that do not support Weber’s law suggest that contrast discrimination follows a power function over the

rising part of the TvC curve and that the gradient is less than 1. Estimates of the values of the exponent in the power law relation vary between 0.5 and 1. We attempt to show that such estimates provide a less than satisfactory way to discriminate among models of contrast discrimination.

Another interesting result with some implications for theories of contrast discrimination is the fact that the psychometric functions for a fixed pedestal contrast do not have the same form.^{2,7,17} [The occurrence of steep detection psychometric functions (pedestal contrast of 0), compared with the shallow discrimination functions where discrimination is best, led to the suggestion that the pedestal effect might reflect a reduction in signal uncertainty—a pedestal may specify the spatial frequency, duration, location, and, in some cases, the phase of the signal that is to be detected.^{9,15}] We attempt to show that estimates of the slopes of the psychometric functions also provide a less than satisfactory way to discriminate among models of contrast discrimination.

Because the psychometric functions are not parallel on semilogarithmic coordinates, the shape of the TvC function depends on the performance level chosen to represent the threshold.^{7,17} It has also been shown¹⁷ that the slopes of the linear portion of the TvC are affected by stimulus duration; at short (20-ms) and at long (1497-ms) durations, the data appeared to be fitted better by Weber's law than at intermediate (79-ms) presentation times.

The present study uses standard temporal 2AFC procedures to explore the TvC function for sinusoidal gratings of different spatial frequency presented at a duration (79 ms) that is unfavorable to the production of Weber's law.

2. METHOD

Two observers, the authors CMB and GBH, served in 2AFC detection and contrast-discrimination experiments. The stimuli to be detected, the signals, were horizontally orientated sinusoidal gratings with spatial frequencies ranging from 2.03 to 16.2 cycles per degree of visual angle (c/deg). The signals were presented either for detection, i.e., against uniform fields of the same mean luminance as the signal (88.5 cd/m²), or for discrimination, i.e., against background gratings of the same mean luminance. The background gratings, sometimes called "maskers" and sometimes called "pedestals," consisted of gratings of the same orientation, spatial frequency, and phase as the signal. The masker and the signal were simultaneously gated on and off inside a rectangular temporal envelope of 78.8-ms duration, and they were presented within the same circularly symmetric Hanning spatial window with a radius subtending 2.1 deg of visual angle at the viewers' eyes. (An additional stimulus, called the 0.0-c/deg grating, comprised a uniform field of adjustable luminance within the Hanning window.)

The two 78.8-ms observation intervals of each trial were separated by a 750-ms pause. In the detection experiments, a signal grating of a given spatial frequency and contrast was presented in one interval. The other interval contained a uniform field of the same mean luminance. The observers were required to indicate which interval had contained the signal by pressing buttons dur-

ing the 1.0-s answer interval that followed the second observation interval. The signal appeared in the first interval of each trial with probability 0.5. Tones marked the beginning and end of each observation interval and, after the 1.0-s response interval, tones indicated the interval that had contained the signal.

In the discrimination experiments, a masker or pedestal grating of the same spatial frequency and phase as the signal and of fixed contrast was presented in both observation intervals, and the signal was added in one of the intervals. (The detection experiment is thus just a discrimination experiment with a pedestal of zero contrast.) With the exception of the 0.0-c/deg stimulus, presentation of the pedestal grating, the signal grating, or their sum did not change the mean luminance of the display.

The phase of the pedestal with respect to the spatial window changed randomly from observation interval to observation interval; one of eight phases (uniformly distributed over 2π rad) was chosen for each presentation. The phase of the signal was the same as that of the pedestal so that the signals were always added in the same phase as the pedestals.

The contrasts of both the pedestal and the signal were fixed for blocks of 50 trials after which the contrast of the signal was changed in order to determine 5- or 6-point psychometric functions relating the proportion of correct responses to signal contrast. The pedestal contrast was then changed and the process repeated for a range of seven or eight background contrasts (including zero, for detection), and then the spatial frequency of the stimulus was changed. Finally, the entire experiment was repeated in a different order so that the psychometric functions for each observer, each spatial frequency, and each background contrast were ultimately based on five or six observations of 100 points each.

The stimuli were generated in MATLAB as floating-point arrays, converted to an integer representation and then written to the green gun of a suitably linearized Mitsubishi FR8905SKHKL display by combining the output of three 8-bit digital-to-analog converters through a linear network.^{17,18} The arrangement provided a dynamic luminance range of ~ 12 bits. Stimuli were presented at a frame rate of 152 Hz (with no interleaving), and the linearity of the CRT was assessed with a digital camera (Photometrics SenSys 200 KAF 0400) to ensure that any distortion introduced by the display was negligible.¹⁷

All experimental stimuli were presented as a 256×256 -pixel array using the central 46% of the display. Each side of the square measured 17.2 cm in length so that the pixel size on the screen was 0.67 mm². The screen was viewed binocularly with natural pupils at a distance of 234 cm. Thus the central square subtended 4.2×4.2 deg of visual angle at the observers' eyes, and each pixel subtended approximately 1 arc min of visual angle. The pixels surrounding the central square were set to the mean luminance of the display (88.5 cd/m²).

3. RESULTS AND DISCUSSION

Figures 1(a) and 1(b) show psychometric functions separately for each observer; the proportion of correct responses (linear) is plotted as a function of signal contrast (logarithmic). The spatial frequency of the stimuli was

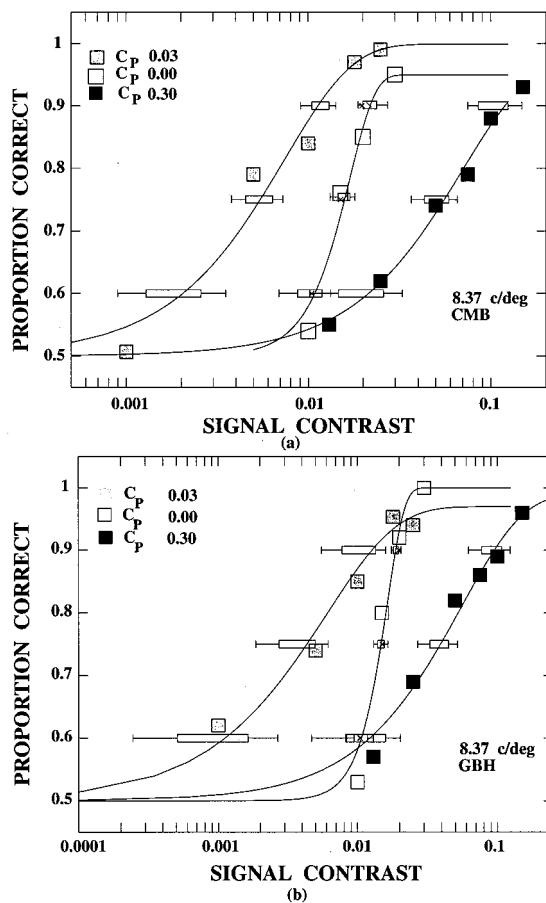


Fig. 1. (a) Proportion of correct responses (linear) as a function of signal contrast (logarithmic) for 8.37-c/deg stimuli. The results are for observer CMB, and each observation point is based on 100 observations. Results are shown for pedestal contrasts of 0% (detection, open squares), 30% (black squares), and 3.25% (gray squares). The smooth curves are the best-fitting three-parameter Weibull functions.^{19,20} (b) Identical to (a), but for observer GBH.

8.37 c/deg, and results for pedestal contrasts of 0% or detection (open squares), 30% (black squares), and 3.25% (gray squares) are shown. Each data point is based on 100 observations, and the smooth curves through the points are the best-fitting three-parameter Weibull functions. The horizontal lines and boxes at 60%, 75%, and 90% correct indicate the 95% and 68% confidence intervals for the corresponding signal contrasts, respectively. Like the fitted Weibull functions, they were obtained with the bootstrap procedure of Wichmann and Hill.^{19,20}

There are a number of features to note. First, the smooth curves giving the best (maximum-likelihood) fits do not all asymptote at 100% correct responses. This is most noticeable in the detection function for CMB. The asymptote reflects what Wichmann and Hill model in their fitting procedure as a "lapse rate." Failure to include a lapse-rate parameter in the fitting procedure can lead to serious mis-estimates of thresholds and particularly slopes.^{19,20} Second, it is obvious that the psychometric functions are not parallel on these coordinates; as has been noted in previous studies, the detection functions are considerably steeper than the other two.^{7,14,17} The

mean slope of the detection functions at 75% correct for the two observers on these coordinates is 2.63, whereas that for the four discrimination functions is 0.83. Although there are a number of important technical problems,²¹ the bootstrap procedure of Wichmann and Hill provides confidence intervals for estimates of the slopes. For each observer, the slope estimates for the two discrimination functions fall within each other's 68% confidence interval; the slopes are, in effect, within one standard deviation of each other. The slopes for the detection functions, however, lie beyond the 95% confidence intervals, and standard hypothesis testing techniques would allow us to reject the hypothesis that the detection function has the same slope as the discrimination functions.

Finally, the psychometric functions appear to touch at the higher performance levels, particularly for GBH. Consequently, there is no transformation of the contrast axis that can make them parallel.²² Thus the shape of the function relating the threshold signal contrast to pedestal contrast must change depending on the performance level chosen to indicate the threshold. For example, a pedestal contrast of 3.25% leads to little improvement over detection performance at the 90% correct level, but performance is nearly an order of magnitude better with the 3.25% pedestal than in detection at the 60% correct level.

To make the effect of different choices of threshold clear, Fig. 2 shows the well-known pedestal effect or "dipper" function obtained at three different performance levels. Because the pedestal and the signal have the same frequency and phase, the addition of the signal in one observation interval simply causes an increase in the stimulus contrast in that interval. The ordinate can thus be labeled either "signal contrast" or "contrast increment" because the size of the contrast increment for in-phase addition is just the signal contrast.

Figure 2 shows, separately for each observer, the signal contrasts corresponding to 90%, 75%, and 60% correct as a function of pedestal contrast; both axes are logarithmic, and the grating frequency is 2.09 c/deg. (For convenience, the results from the detection condition, zero pedestal contrast, are arbitrarily plotted at a contrast of 0.0001%. The error bars show 95% confidence intervals derived from Wichmann and Hill's bootstrap procedure.^{19,20}

Our results are consistent with those of Wichmann¹⁷ and the inference from Fig. 1: The shapes of the function are different for different thresholds. The initial improvement in performance with increasing pedestal level is greater at the 60% level than at the 75% level and is almost nonexistent at the 90% level.

At each pedestal level the separation between the contours of constant performance indicates the slope of the psychometric functions plotted on semilogarithmic coordinates. Consistent with Fig. 1, they are steepest at a pedestal contrast of 0 (detection) and shallowest near the best performance where the pedestal effect is greatest and the dip in the dipper is lowest. Above the pedestal contrast that produces the best performance, the contours are approximately parallel, and their slope is an indication of whether Weber's law holds.

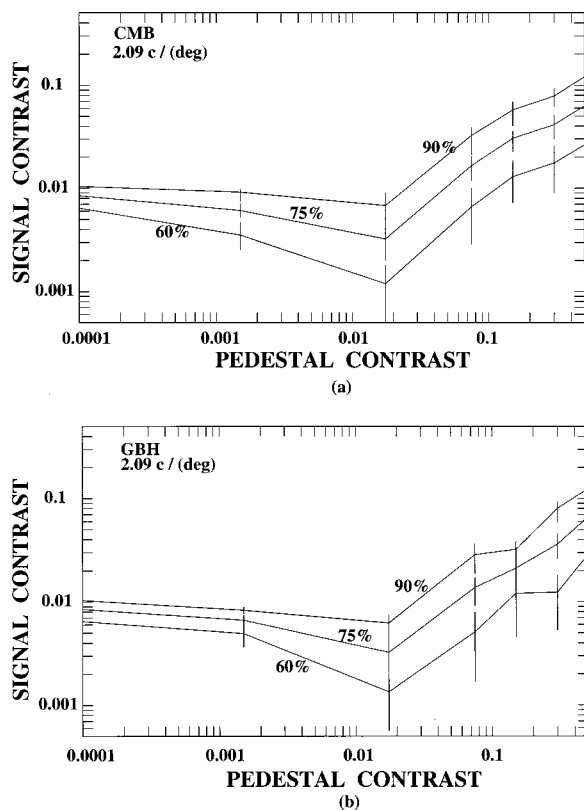


Fig. 2. (a) Signal contrast corresponding to 90%, 75%, and 60% correct as a function of pedestal contrast; both axes are logarithmic, and the spatial frequency of the grating is 8.37 c/deg. (For convenience, the result from the detection condition, 0 pedestal contrast, is arbitrarily plotted at a contrast of 0.0001.) The results are derived from fits to 4–5-point psychometric functions (100 observations per point) for observer CMB. The error bars show 95% confidence intervals.^{19,20} (b) Identical to (a), but for observer GBH.

The steepness of the psychometric functions depends on several factors, e.g., the shape of the underlying space and the parameter that is varied so as to trace out the psychometric function. We return to this issue in Section 4.

In order to present the data for all spatial frequencies, we first normalized the pedestal contrast and the contrast increment at each frequency. As the normalizing factors at each spatial frequency, we used for each observer the best estimate of the contrast that corresponded to 75% correct detection (i.e., that obtained at a pedestal level of 0). The estimates for CMB, together with their mean 95% confidence intervals, were 0.021 ± 0.002 , 0.008 ± 0.001 , 0.0095 ± 0.0008 , 0.015 ± 0.002 , and 0.044 ± 0.005 , at 0.0, 2.09, 4.18, 8.37, and 16.74 c/deg, respectively, and for GBH they were 0.025 ± 0.002 , 0.008 ± 0.001 , 0.010 ± 0.002 , 0.015 ± 0.002 , and 0.048 ± 0.003 , at the same spatial frequencies.

The detection results indicate that from 2 to 16 c/deg, performance is a monotonic decreasing function of spatial frequency. This result is consistent with the usual observations with stimuli of high temporal frequency.^{23,24} At our 78.8-ms duration, however, performance is worse with the uniform field (0-c/deg grating) than with the 2-c/deg grating.

The three rows of Fig. 3 show the normalized contrast increment (or signal contrast) corresponding to 60%, 75%, and 90% correct responses as a function of normalized pedestal contrast. The left-hand column shows the results for CMB, the right-hand column for GBH.

Results for five different spatial frequencies are shown in each panel: 2.09 c/deg (circles), 4.19 c/deg (triangles), 8.37 c/deg (squares) and 16.74 c/deg (diamonds). The results for the uniform-field (or 0.00-c/deg) condition are indicated by an asterisk. Both axes are logarithmic, and the error bars correspond to the 95% confidence interval at the appropriate performance level.^{19,20}

Consider first Fig. 3(b) (75% contours). With the normalized data, the detection thresholds map to 1 and the deepest part of the TvC function occurs at a pedestal contrast of approximately twice this value at all spatial frequencies. The shape of normalized functions are virtually independent of spatial frequency (even at 0.00 c/deg); in particular, the slopes at high contrast depend very little on spatial frequency.

Although the shapes of the TvC functions change with the performance used to define the threshold [Figs. 3(a) and 3(c)], the shapes of the functions for different spatial frequencies at a given performance level again appear similar. The pedestal contrast producing the smallest threshold lies above the detection threshold in all cases, and the slopes of the functions above their lowest points do not depend much on spatial frequency. The magnitude of the dip below the detection threshold is greatest at the lowest (60%) performance level and very small at the 90% level. Above the contrast corresponding to the best performance, the magnitude of the signal or contrast increment producing a given performance level is very similar at all the frequencies we used.

We tested whether any of the slopes at the high-contrast end of the TvC functions depended on spatial frequency by performing simple linear regressions using the points on the rising portion of the function for all three threshold levels for each observer separately.

Table 1 shows the slopes with their 95% confidence intervals.²¹ The slope depends on how much of the TvC function is included. Except at 16 c/deg, we were able to include four points; at 16 c/deg, only three were clearly on the rising part of the TvC curves. NS in the table indicates that the regression was not significant—too few points at 16 c/deg and data too variable in the other two cases—and these entries should be ignored.

As the thresholds decrease from 90% to 75% to 60% correct, the slopes for GBH, on average, increase from 0.78 to 0.81 to 1.03, and for CMB, they increase from 0.91 to 0.96 to 1.01. This effect is not statistically significant. There is a very slight tendency for gratings of lower spatial frequency to have a shallower slope, at least for our brief 78.8-ms durations, but, taken across the two observers, the results are not inconsistent with Weber's law (slope 1) at all the spatial frequencies we used. (The confidence limits for the slopes at the 60% threshold were always greater than at the other two thresholds. The confidence limits at the 75% and 90% thresholds were similar. Both features are a result of the binomial variability in the number of correct responses reflected through psychomet-

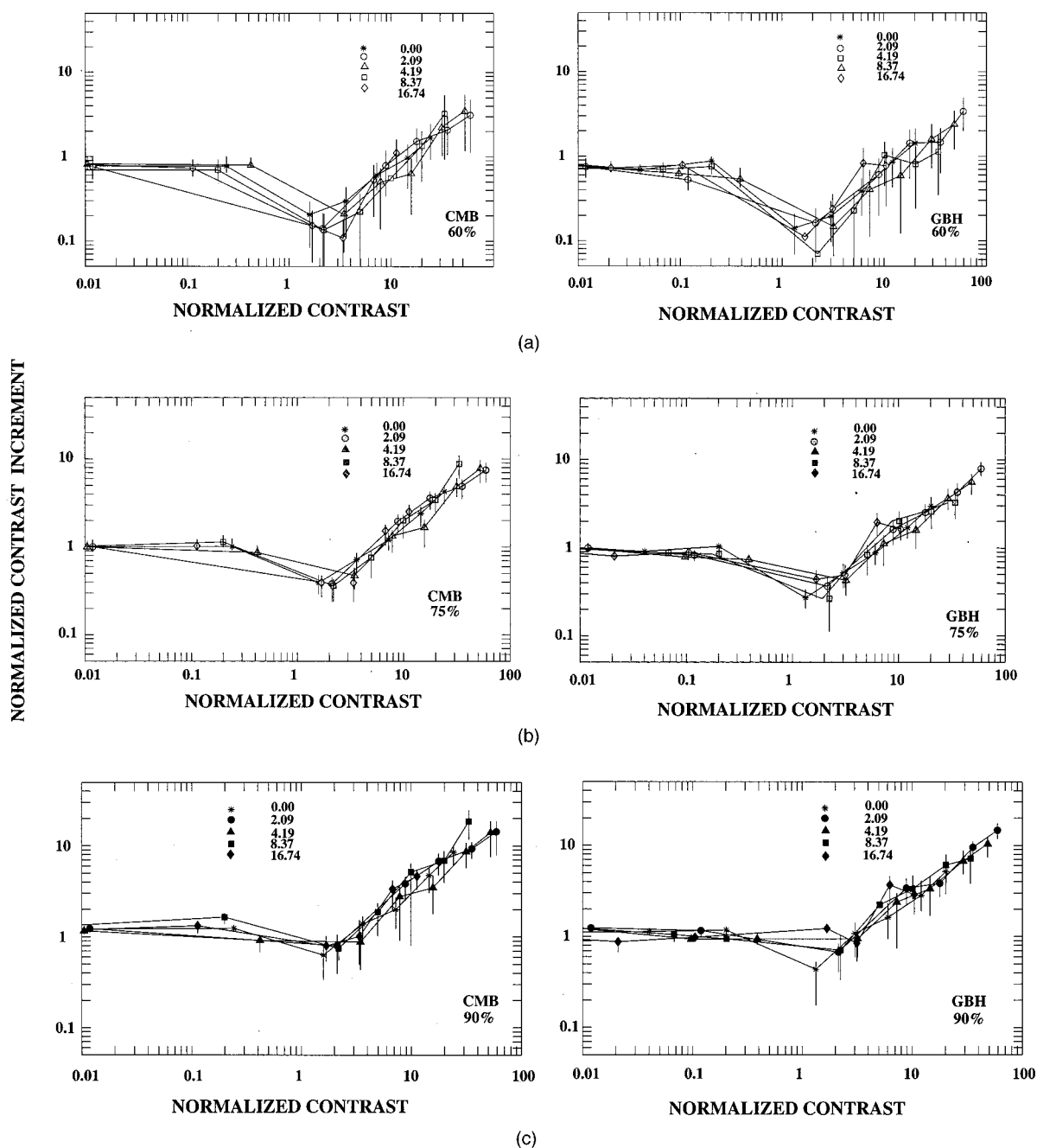


Fig. 3. Normalized contrast increment (or normalized signal contrast) as a function of normalized pedestal contrast. The three rows show the normalized contours for 60%, 75%, and 90% correct, for stimuli of five different spatial frequencies: 2.09 c/deg (circles), 4.19 c/deg (triangles), 8.37 c/deg (squares), and 16.74 c/deg (diamonds). The uniform field or 0.0-c/deg results are shown as asterisks. Both axes are logarithmic. The normalization factors for each spatial frequency, the contrasts corresponding to the 75% correct detection condition, zero pedestal contrast, were used for both axes and all three performance contours. (For convenience, the result from the detection condition, zero pedestal contrast, is plotted at an arbitrarily low but nonzero pedestal contrast.) The error bars show 95% confidence intervals.^{19,20} The left-hand column shows the results for CMB, the right-hand column for GBH.

ric functions the slopes of which differ at different performance levels; see Fig. 1.)

Legge²⁵ proposed a power law with an exponent of 0.65 to underlie contrast discrimination. Swift and Smith³ also concluded that when observers are highly familiar with the masking stimuli used, thresholds vary as the 0.65 power of the masker contrast. They suggested that when observers are well practiced with a particular masker, they cease to base comparisons on the actual ap-

pearance of the gratings to be discriminated and detect the signal by looking for deviations from the expected appearance of the masker alone. In the present study, the observers reported looking for different cues in the stimuli at different spatial frequencies. At some spatial frequencies, for example, it was easier to compare a few bright and dark bands in the center of the display, while at others it was easier to compare the overall dark appearance of the dark bars. The use of such different

Table 1. Slopes and [95% Confidence Intervals]

Spatial Frequency (deg)		GBH	CMB
0	60%	1.05 [0.68, 1.45]	0.87 [0.55, 1.30]
	75%	0.90 [0.70, 1.20]	0.92 [0.68, 1.15]
	90%	0.80 [0.58, 1.08]	0.95 [0.68, 1.20]
2	60%	^{NS} 0.81 [0.45, 1.25]	0.65 [0.25, 1.15]
	75%	0.80 [0.64, 1.05]	0.67 [0.52, 0.90]
	90%	0.85 [0.66, 1.20]	0.65 [0.57, 1.05]
4	60%	1.00 [0.60, 1.45]	1.12 [0.75, 1.58]
	75%	0.90 [0.70, 1.15]	1.00 [0.8, 01.30]
	90%	0.85, [0.60, 1.05]	0.92 [0.75, 1.25]
8	60%	^{NS} 0.68 [0.25, 1.25]	1.39 [0.85, 1.95]
	75%	0.65 [0.35, 0.97]	1.23 [1.07, 1.58]
	90%	0.63 [0.30, 1.00]	1.10 [0.97, 1.58]
16	60%	^{NS} 1.07 [0.25, 1.70]	^{NS} 1.97 [1.25, 2.85]
	75%	^{NS} 1.25 [0.67, 1.39]	^{NS} 1.57 [1.05, 1.92]
	90%	^{NS} 1.15 [0.65, 1.50]	^{NS} 1.27 [0.58, 1.55]

NS, not significant.

cues, however, did not result in significant deviations from Weber's law, despite extensive training at all the spatial frequencies we used.

The most recently published study to investigate contrast discrimination at a number of spatial frequencies was reported by Bradley and Ohzawa.²⁶ We have tried, as far as is possible, to compare our results with theirs. They found slopes of ~ 0.9 for most spatial frequencies, although their slope for stimuli of 0.5 c/deg was 0.7. These results are in reasonable agreement with the results presented above. Bradley and Ohzawa²⁶ concluded that spatial frequency has little effect on suprathreshold contrast discrimination; the present study with stimuli of 78.8-ms duration is not inconsistent with that conclusion.

A fixed signal level leads inescapably to at least binomial variability in the number of correct responses at each point. That variability is reflected in the confidence that can be placed in both the threshold and the slope estimates.²¹ This in turn affects the confidence intervals of derived characteristics such as the slope of the rising part of the TvC functions. Even with conventional regression analysis, the confidence intervals for that characteristic are very wide. This, then, has major implications for studies attempting to differentiate among laws governing the behavior of the rising portion of the TvC function. The results presented above show that this issue, as far as our experiments go, is basically academic. Because of the widths of the confidence interval for slopes, nearly all of GBH's slopes could be explained either by Weber's law or by a power law with exponent of 0.65 (CMB's results are better fitted by Weber's law). To argue for a compressive nonlinearity in suprathreshold contrast discrimination from the slopes of the rising part of the TvC curves, then, it must be made clear that these slopes are significantly less than 1. This is certainly not the case here. In the light of these results it would seem that further research trying to characterize contrast dis-

crimination should concentrate not simply on the rising portion of the TvC function but on the whole of the function. This would place more constraints on the models to be tested.^{11,17,21}

4. GENERAL DISCUSSION

One helpful way of considering the results of pedestal- or contrast-discrimination experiments is to represent the data in a different coordinate system.¹⁰ In Fig. 4, relative contrast of the stimuli in the two intervals is plotted on the ordinate, and the contrast (or signal-to-noise ratio) of the higher-contrast signal is plotted on the abscissa. Both axes are logarithmic. For our conditions, with signal and pedestal added in phase, $(c_s + c_p)/c_p$ appears on the ordinate and $c_s + c_p$ on the abscissa, where c_s and c_p are the contrasts of the signal and the pedestal, respectively. Figure 4 indicates the form that the results, including ours, usually take.

In terms of the representation in Fig. 4, increasing the pedestal level while keeping the signal level fixed increases the detectability of the stimuli in both observation intervals (by increasing their signal-to-noise ratio) but reduces the discriminability of the stimuli (by reducing their ratio). Thus the axes of the figure provide a rough and ready way of representing detectability on the x axis and discriminability on the y axis. The figure does not, of course, explain the results, but any model that predicts the shape of this surface will capture all the results of our experiments.^{10,11,17}

The roughly hyperbolic lines are contours of constant performance so that the space looks like the corner of an escarpment with a high plateau of good performance above a plane of poor performance. Psychometric functions are paths up the escarpment. Psychometric functions obtained, as in our experiments, by varying the signal contrast but keeping the pedestal contrast fixed yield paths that all lie along lines at an angle of 45°. When the

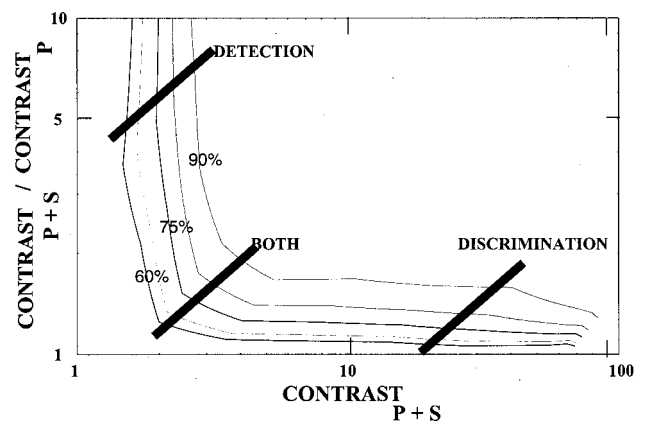


Fig. 4. Form in which data from Fig. 3 appear when the relative contrast of the signal-plus-pedestal to that of the pedestal alone is plotted against the contrast of the signal-plus-pedestal on logarithmic coordinates. The fine lines show contours of constant performance. In experiments performed with fixed pedestal contrast and increasing signal contrast, the usual psychometric functions move upward over the underlying surface at an angle of 45° (along the thick bars). (The data from which Fig. 4 derives are for observer GBH and 8.37-c/deg gratings from Ref. 11.

pedestal contrast is small (as in the top left-hand corner) steep detection psychometric functions are obtained because the underlying performance contours are closely packed. Yet steeper functions could be obtained in this region by increasing both signal and pedestal contrast together so that the path up the escarpment lies parallel to the x axis and along the local gradient of the underlying space.

When the pedestal level is high (as in the bottom right-hand corner) the psychometric functions for discrimination can also be made steeper by keeping the sum of the signal and (in-phase) pedestal contrast fixed while changing their relative values. The path over the underlying surface would then be parallel to the y axis and again along the local gradient. Where performance is improved by the pedestal, i.e., near the corner of the escarpment at the lowest point in the TvC function, the gradient of the underlying space is near the 45° line so that the shallow psychometric functions obtained there are already as steep as possible. They are shallow there because the contours of constant performance in this region are widely spaced even along the gradient. The figure indicates that the slopes of the psychometric functions will depend on the way in which they are obtained. Thus it is important, from a theoretical point of view, to model the underlying space rather than psychometric functions the characteristics of which depend both on shape of the underlying space and on the path taken over the underlying space in generating the psychometric functions.

ACKNOWLEDGMENTS

The research was carried out in the Sensory Research Unit, Oxford University, and was supported by grants from the Wellcome Trust to G. B. Henning and F. A. Wichmann and by a Fellowship by Examination at Magdalen College, Oxford University (F. A. Wichmann).

REFERENCES

1. F. W. Campbell and J. G. Robson, "Application of Fourier analysis to the visibility of gratings," *J. Physiol. (London)* **197**, 551–556 (1968).
2. G. E. Legge and J. M. Foley, "Contrast masking in human vision," *J. Opt. Soc. Am.* **70**, 1458–1471 (1980).
3. D. J. Swift and R. A. Smith, "Spatial frequency masking and Weber's law," *Vision Res.* **23**, 495–505 (1983).
4. G. B. Henning, B. G. Hertz, and D. E. Broadbent, "Some experiments bearing on the hypothesis that the visual system analyses patterns in independent bands of spatial frequency," *Vision Res.* **15**, 887–899 (1975).
5. A. M. Derrington and G. B. Henning, "Some observations on the masking effects of two-dimensional stimuli," *Vision Res.* **29**, 241–246 (1989).
6. F. W. Campbell and J. J. Kulikowski, "Orientation selectivity of the human visual system," *J. Physiol. (London)* **187**, 437–445 (1966).
7. J. Nachmias and R. V. Sansbury, "Grating contrast: discrimination may be better than detection," *J. Physiol. (London)* **14**, 1039–1042 (1974).
8. B. Leshowitz and D. H. Raab, "Effects of stimulus duration on the detection of sinusoids added to continuous pedestals," *J. Acoust. Soc. Am.* **41**, 489–496 (1967).
9. D. M. Green and J. A. Swets, *Signal Detection Theory and Psychophysics* (Wiley, New York, 1966).
10. G. B. Henning, "Amplitude discrimination in noise, pedestal experiments, and additivity of masking," *J. Acoust. Soc. Am.* **45**, 426–435 (1969).
11. F. A. Wichmann, G. B. Henning, and A. C. Ploghaus, "Non-linearities and the pedestal effect," *Perception* **27**, S86 (1998).
12. J. J. Kulikowski and P. E. King-Smith, "Spatial arrangement of line, edge and grating detectors revealed by sub-threshold summation," *Vision Res.* **13**, 1455–1478 (1973).
13. D. M. Green, "Psychoacoustics and detection theory," *J. Acoust. Soc. Am.* **32**, 1189–1203 (1960).
14. J. M. Foley and G. E. Legge, "Contrast detection and near-threshold discrimination in human vision," *Vision Res.* **21**, 1041–1053 (1981).
15. D. G. Pelli, "Uncertainty explains many aspects of visual contrast detection and discrimination," *J. Opt. Soc. Am. A* **2**, 1508–1532 (1985).
16. J. M. Foley, "Human luminance pattern-vision mechanisms: masking experiments require a new model," *J. Opt. Soc. Am. A* **11**, 1710–1719 (1994).
17. F. A. Wichmann, "Some aspects of modelling human spatial vision: contrast discrimination," D. Phil. thesis, Oxford University, Oxford, UK, 1999.
18. D. G. Pelli and L. Zhang, "Accurate control of contrast on microcomputer displays," *Vision Res.* **31**, 1337–1350 (1991).
19. F. A. Wichmann and N. J. Hill, "The psychometric function I: fitting, sampling and goodness-of-fit," *Percept. Psychophys.* **63**, 1293–1313 (2001).
20. F. A. Wichmann and N. J. Hill, "The psychometric function II: bootstrap-based confidence intervals and sampling," *Percept. Psychophys.* **63**, 1314–1329 (2001).
21. N. J. Hill, "Testing hypotheses about psychometric functions: an investigation of some confidence interval methods, their accuracy, and their use in evaluating optimal sampling strategies," D. Phil. thesis, Oxford University, Oxford, UK, 2001.
22. M. V. Levine, "Transformations that render curves parallel," *J. Math. Psychol.* **7**, 410–443 (1970).
23. J. G. Robson, "Spatial and temporal contrast-sensitivity functions of the visual system," *J. Opt. Soc. Am.* **56**, 1141–1142 (1966).
24. D. H. Kelly, "Flickering patterns and lateral inhibition," *J. Opt. Soc. Am.* **59**, 1361–1370 (1969).
25. G. E. Legge, "A power law for contrast discrimination," *Vision Res.* **21**, 457–467 (1981).
26. A. Bradley and I. Ohzawa, "A comparison of contrast detection and discrimination," *Vision Res.* **26**, 991–997 (1986).